Optics Communications 412 (2018) 150–154

Contents lists available at ScienceDirect

Optics Communications

journal homepage: www.elsevier.com/locate/optcom

Multi-resonance peaks fiber Bragg gratings based on largely-chirped structure

Chao Chen [a,*], Xuan-Yu Zhang [b], Wei-Hua Wei [b], Yong-Yi Chen [a], Li Qin [a], Yong-Qiang Ning [a], Yong-Sen Yu [a,*]

[a] State Key Laboratory of Luminescence and Application, Changchun Institute of Optics, Fine Mechanics and Physics, Chinese Academy of Sciences, Changchun 130033, China

[b] State Key Laboratory on Integrated Optoelectronics, College of Electronic Science and Engineering, Jilin University, Changchun 130012, China

ARTICLE INFO

Keywords:
Femtosecond laser
Fiber Bragg gratings
Optical fiber sensors
Fiber optics

ABSTRACT

A composite fiber Bragg grating (FBG) with multi-resonance peaks (MRPs) has been realized by using femtosecond (fs) laser point-by-point inscription in single-mode fiber. This device contains a segment of largely-chirped gratings with the ultrahigh chirp coefficients and a segment of uniform high-order gratings. The observed MRPs are distributed in an ultra-broadband wavelength range from 1200 nm to 1700 nm in the form of quasi-period or multi-peak-group. For the 8th-order MRPs-FBG, we studied the axial strain and high-temperature sensing characteristics of different resonance peaks experimentally. Moreover, we have demonstrated a multi-wavelength fiber lasers with three-wavelength stable output by using a 9th-order MRPs-FBG as the wavelength selector. This work is significant for the fabrication and functionalization of FBGs with complicated spectra characteristics.

1. Introduction

Fiber Bragg grating (FBG) has narrow band filtering characteristics at certain wavelength, which becomes important devices for fiber sensing [1], fiber laser [2–4] and fiber communication [5]. Aiming at the demands in special fields of multi-parameter sensing and wavelength division multiplexing, the researchers have developed multiple FBGs with multi-resonance peaks (MRPs), such as superimposed-[6], superstructure-[7], cascaded-[8] and multi-core-[9] FBG. As for these grating structure, the conventional UV laser writing technique has some drawbacks, such as, the fiber needs to load hydrogen, Bragg resonance wavelength highly depends on the phase mask period, and it is difficult to fabricate large period (high order) Bragg grating. These problems make the fabrication process of the UV-FBG lack of flexibility, which is challenging to realize complex grating structures and expand their functions. In recent years, femtosecond laser directing writing (FsLDW) technique demonstrates obvious advantages in fabrication of FBG [10–16]. The fs laser interacts with dielectric material through high nonlinear photoionization mechanism, leading to the modification which is not related to the photosensitivity of material [12–14]. If we combine this technique with point-by-point (PbP) method, we can control the location of the refractive index (RI) modification in the fiber precisely and flexibly through the fabrication program [14,17–22]. Therefore, fs laser point by point writing technique can fabricate any complex grating structures in principle, which is very important for achieving the FBG with unique spectrum characteristics and functionalities [20].

In this manuscript, we utilize the flexible fs laser PbP writing method and fabricate a kind of composite FBG with MRPs. This composite grating contains a segment of largely-chirped grating with ultra-high chirped coefficient and a segment uniform high-order grating, which is realized through designing the axial location of the RI modulation in the fiber core. In the experiment, we fabricate two kinds of MRPs-FBG, which own multiple narrow band resonances distributed in the forms of quasi-period or multi-peak-group. For the former, we studied the high temperature and axial strain sensing characteristics of the multi-resonances peaks. For the latter, we demonstrate a kind of three wavelength fiber laser utilizing the multiple wavelength selectivity.

2. Experiments

The schematic diagram of the setup for FBG inscription by PbP method with fs laser is shown in Fig. 1(a). Experimentally, a Ti: sapphire regenerative amplifier laser system (Spectra Physics) with the operation wavelength of 800 nm and pulse duration of 100 fs was adopted. The chosen laser repetition (f) and pulse energy are 100 Hz and 75 nJ/pulse,

* Corresponding authors.
E-mail addresses: chenc@ciomp.ac.cn (C. Chen), yuys@jlu.edu.cn (Y.-S. Yu).

https://doi.org/10.1016/j.optcom.2017.12.004
Received 20 September 2017; Received in revised form 21 November 2017; Accepted 1 December 2017
Available online 19 December 2017
0030-4018/

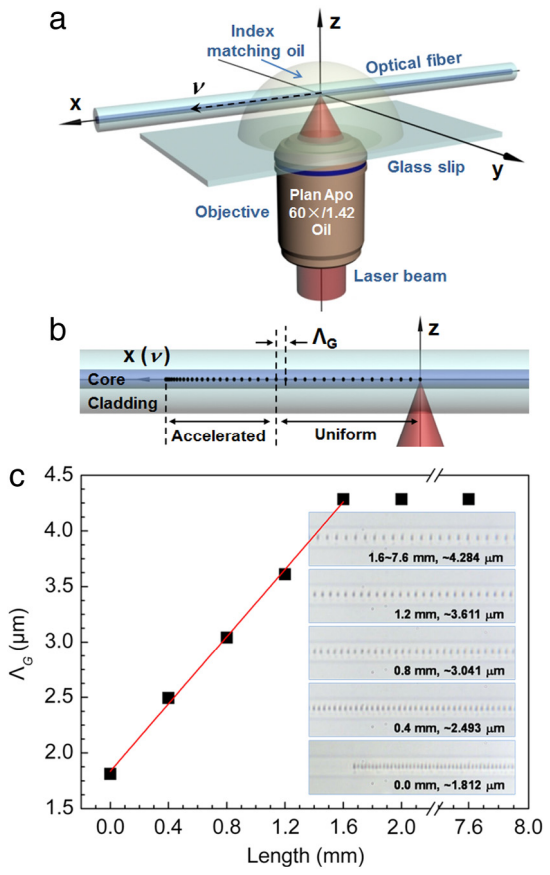

Fig. 1. (a) Schematic diagram of the setup for FBG inscription by PbP method with fs laser. (b) Sketch of the fs-written RI modification array. (c) The gratings period changes with the grating length. Insets: the microscopic grating structures are corresponding to the different locations.

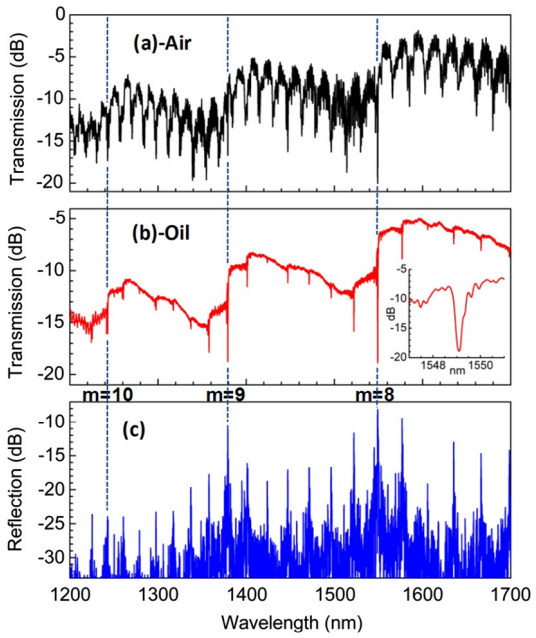

Fig. 2. Spectra of the 8th-order MRPs-FBGs. (a) Transmission spectrum in air. (b) Transmission spectrum in RI matching oil. (c) Reflection spectrum, the inset shows the close-up of the 8th-order major Bragg resonance.

respectively. In order to control the RI modification profiles precisely, the laser beam was firstly filtered through a pin-hole to get rid of noise and form a smooth Gaussian beam with the diameter adjusted to 4 mm. And then, the laser beam was tightly focused into the fiber (Corning SMF-28) in a tiny volume through a high numerical aperture (N.A. = 1.42) 60 × oil-immersion objective to increase the RI modulation. The fiber sample was not photosensitized and was fixed to a high-precision three dimensional translation stage. In order to avoid the focus distortion caused by the fiber cylindrical lens effect, the fiber is immersed in the pine tar with the RI of 1.515 [19–21].

Fig. 1(b) shows the illustration of the fiber moving along X axis during the fabrication process, which contains an acceleration movement segment and a uniform velocity movement segment. In such MRPs-FBG, a segment of chirped grating with ultra-large coefficient (C) and a segment of uniform grating with high-order period (Λ_G) will be formed. In the chirped grating segment, the relationship between the period ($\Lambda(x)$) and the chirped coefficient can be expressed as $\Lambda(x) = \Lambda_0 + C \cdot x$, in which, Λ_0 is the initial period. The chirped coefficient can be achieved with the fiber acceleration, all the FBGs in this paper have the same acceleration value, i.e. 20 μm/s^2. In the uniform grating segment, the period can be expressed as $\Lambda_G = v_G/f$, in which, v_G is the inscription speed of the uniform grating. For the 8th- and 9th-order uniform gratings involved below, the speeds are 428.4 μm/s and 482.0 μm/s, respectively. The grating inscription is controlled by the fabrication program. The inscription program is programmed based on the period of the high order uniform grating and acceleration.

The largely-chirped structure in the composite FBG is comprised of a serial of short length and period increased uniform gratings. The resonance wavelength λ_B can be achieved with the phase matching condition $m\lambda_B(x) = 2n_{eff}(x)\Lambda(x)$, in which, m is the grating order, n_{eff} is the effective RI of the guiding mode. For the grating written by fs laser, when the induced RI modulation is large enough (larger than 10^{-3}), the grating can still produce strong Bragg resonance, even the grating length is only about hundreds of micrometers [23]. Therefore, we can predict that, the spectrum of this unique grating structure will not only show the major Bragg resonance that comes from the uniform grating section, but also present many additional Bragg resonances that result from the largely-chirped section. In experiment, we fabricate two kinds of MRPs-FBG, their multi-resonances are distributed in forms of quasi-period and multi-peak-group, respectively. We will give the representative device and characteristic spectrum in the following paragraph. A broadband light source (Superk Compact, NKT Photonics) and an optical spectrum analyzer (OSA, AQ6370B, Yokogawa) with a wavelength resolution of 0.02 nm are used for characteristic spectrum monitoring.

Fig. 1(c) gives the relationship of the fabricated 8th-order (Λ_G = 4.284 μm) composite grating period changes with the grating length. The inset shows the RI modulation microscope image at different locations. The length of the chirped segment is 1.6 mm, the initial and the final periods are 1.812 μm and 4.284 μm, respectively, and the chirped coefficient is 1545 nm/mm. The length of the uniform grating segment is 6.0 mm. It needs to be declared that the highly localized composite FBGs will excite a strong cladding mode resonance [24–26]. In addition, the Mie scattering derived from micro-void modifications will induce strong broadband scattering loss in the grating [27]. The above spectra characteristics are reflected in the transmission spectrum shown in Fig. 2(a), which is measured in air. The reflection spectrum corresponding to the 8th-order composite grating is shown in Fig. 2(c), as expected, there are other extra six resonance peaks distributed between the two adjacent major Bragg resonances in a quasi-period way, which result from the largely-chirped gratings section. To verify whether they result from the resonances among the fundamental modes of the largely-chirped gratings section, the whole composite grating is immersed in RI matching oil to check whether the extra resonance peaks have changes in intensity and wavelength. The experimental results show that none of the resonance peaks changes, and only the cladding modes in the transmission spectrum are converted to radiation modes. It makes the

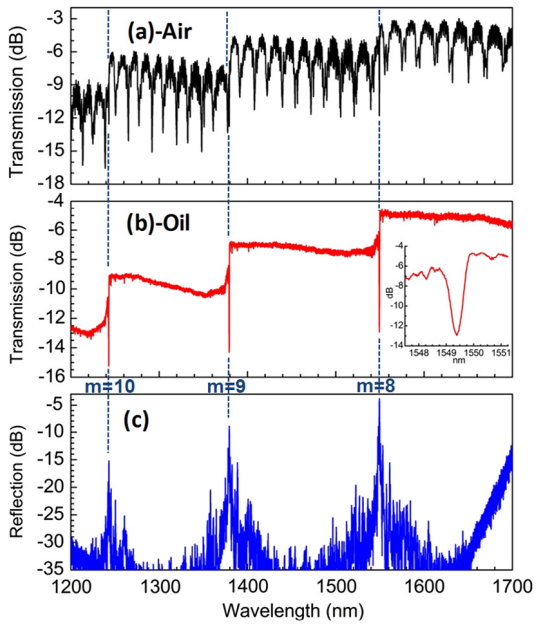

Fig. 3. Spectra of the 8th-order uniform FBGs. (a) Transmission spectrum in air. (b) Transmission spectrum in RI matching oil. (c) Reflection spectrum, the inset shows the close-up of the 8th-order Bragg resonance.

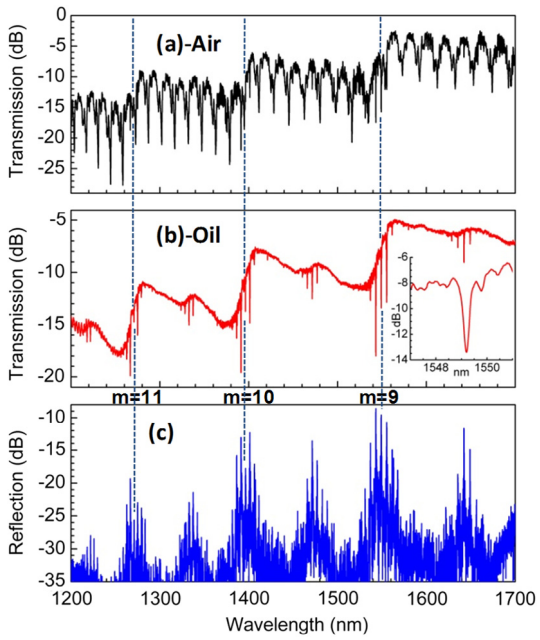

Fig. 4. Spectra of the 9th-order MRPs-FBGs. (a) Transmission spectrum in air. (b) Transmission spectrum in RI matching oil. (c) Reflection spectrum, the inset shows the close-up of the 9th-order major Bragg resonance.

spectrum smooth, and shows a series of resonance peaks corresponded to the reflection spectrum, as shown in Fig. 2(b). Moreover, these extra resonance peaks does not stem from the coupling between the low order cladding modes and the fundamental mode because they are far away from the major Bragg resonance.

To make a comparison, here gives the spectrum characteristics of the 8th-order uniform FBG fabricated with the PbP method. As shown in Fig. 3, it can be seen that the fundamental mode resonances only happen at the wavelength where satisfy the Bragg resonance condition, which correspond to the major Bragg resonances of the 8th-order composite FBG. Therefore, we believe that the largely-chirped gratings section in the composite FBG can bring about novel resonance peaks which differ from the uniform grating in the broadband wavelength range.

Utilizing the same grating inscription method, we also fabricated the MRPs-FBG with grating order smaller than 8th-order and also observed the multi-resonances similar with Fig. 2. However, in the characteristic spectrum of the fabricated 9th-order (Λ_G = 4.820 μm) MRPs-FBG, we observed different characteristic spectrum, as shown in Fig. 4. The MRPs are distributed around Bragg resonance wavelength and in the middle of the adjacent Bragg resonances in the form of multi-peak group (series). The experimental observed distribution status of these two kinds of multi-resonance peaks may be related to the ultra-large chirped grating segment, the deep reason will be studied in the following work.

3. Applications and discussion

3.1. Axial strain and temperature sensing characteristics

We experimentally investigated the axial strain and temperature sensing characteristics of an 8th-order MRPs-FBG. In the experiment, the resonance peaks between 8th- and 9th-order major Bragg resonances were monitored and studied.

The measurement of axial strain was carried out through applying axial tension on the FBG at room temperature. The tension was added from 0 to 1.5 N. Axial strain in the fiber can be obtained by the formula $\varepsilon = F/\pi r^2 E$, where F is the axial tension, r is the cladding radius, and E is the silica Young modulus. The experimental results are shown in Fig. 5. Fig. 5(a) presents the axial strain response for the 8th-order

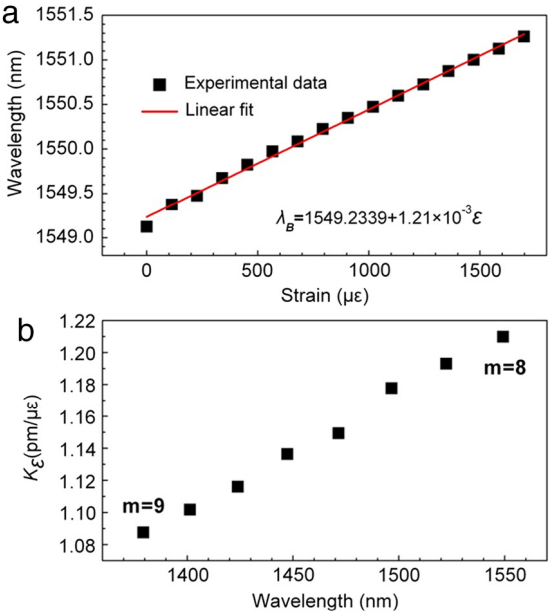

Fig. 5. Axial strain sensing characteristics of the 8th-order MRPs-FBG. (a) Strain response for the 8th-order major Bragg resonant wavelength. (b) Strain sensitivities for different resonant peaks.

major Bragg resonant wavelength. Its linear fitting result shows the strain sensitivity is about 1.21 pm/με. The axial strain sensitivities (K_ε) for different resonant peaks between 8th- and 9th-order major Bragg resonances are shown in Fig. 5(b). The strain responses for each resonant peak are different.

The temperature sensing results for the 8th-order MRPs-FBG are shown in Fig. 6. The temperature increased from room temperature to 1000 °C. Fig. 6(a) shows the linear response of temperature measurement for the 8th-order major Bragg resonant peak. Its temperature sensitivity is 13.41 pm/°C. The temperature sensitivities (K_T) for the

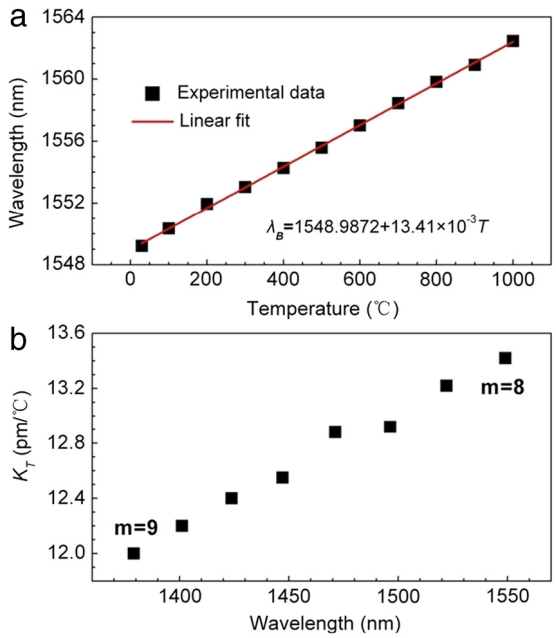

Fig. 6. Temperature sensing characteristics of the 8th-order MRPs-FBG. (a) Temperature response for the 8th-order major Bragg resonant wavelength. (b) Temperature sensitivities for different resonant peaks.

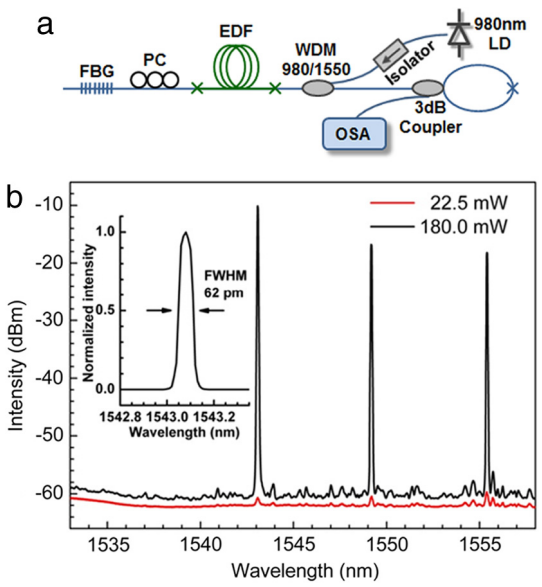

Fig. 7. (a) Experimental setup of the MWFL based on 9th-order MRPs-FBG reflector. (b) Measured output spectrum of the MWFL at the pump power of 22.5 mW and 180.0 mW. The inset shows the linewidth of the laser at 1543.080 nm lasing wavelength.

8 different resonant peaks are shown in Fig. 6(b). Like the strain sensitivities, they are also different from each other.

3.2. The multi-wavelength fiber lasers

The PbP FBGs have been reported to be used for fiber lasers based on the advantages of high temperature stable high power laser output and polarization selectivity [14,28,29]. To expand the functionality of the composite MRPs-FBG, we just shows the possibility of its application in multi-wavelength fiber laser (MWFL) here, and the in-depth research will be carried out in the follow-up work. We fabricated a MWFL operating in C-band with a 9th-order MRPs-FBG. The layout of the fiber laser is shown in Fig. 7(a). The MRPs-FBG is used as a wavelength selector, and a fiber loop mirror is used for the broadband reflecting mirror, they together form the linear-cavity configuration. A section of 3 m-length erbium-doped fiber (EDF) is spliced in the laser cavity as the gain medium. A laser diode (LD) with the operation wavelength of 980 nm is used for pumping the active EDF through a 980/1550 wavelength division multiplexer (WDM). It should be noted that if the pump light inputs from the left side of the MRPs-FBG, lots of the pump energy will attenuate due to the Mie scattering loss in micro-void modifications [27,30].

Because the PbP FBG was polarization sensitive, the reflection peaks intensity could be changed by adjusting the polarization controller (PC) in the laser cavity. The polarization hole-burning effect would suppress the mode competition induced by homogeneous gain broadening, realizing a stable three-wavelength output in the C-band at room temperature. The pump threshold of the fiber laser was about 22.5 mW. The recorded laser spectrum at the pump power of 180.0 mW is shown in Fig. 7(b). Its output wavelengths are 1543.080 nm, 1549.182 nm and 1555.401 nm, respectively. The fiber laser operated on the three lasing peaks mainly due to the corresponding wavelengths simultaneously have the relatively high reflectivities and gains. The lasing peak located at 1543.080 nm has a maximum extinction ratio of ~48 dB. Its normalized spectrum is presented in the inset. The corresponding full width at half maximum (FWHM) is 62 pm.

To improve the output features of the MWFLs, the Bragg gratings could be directly written in the rare earth doped fibers, overcoming the influence on the output light intensity from mismatched fiber splicing [29]. Moreover, the performance of high power fiber lasers based on the MRPs-FBG will be enhanced if the grating has a higher reflectivity, which can be realized when an optimal pulse-energy range is chosen in the fabrication process [30].

4. Conclusion

In conclusion, we have implemented a composite high-order FBG with MRPs by fs laser and PbP method. The MRPs-FBG is consisted of a segment of largely-chirped grating and a segment of uniform high-order grating. The presented multi-resonance peaks are distributed in forms of quasi-period or multi-peak-group in the broad spectrum range from 1200 nm to 1700 nm. In that wavelength range, twenty distinct reflection peaks are observed for an 8th-order MRPs-FBG. Its axial strain and temperature sensing characteristics for different resonant peaks are investigated experimentally. In addition, we have demonstrated a MWFL with stable three-wavelength output by using a 9th-order MRPs-FBG as the wavelength selector. This work is significant for fabrication of FBGs with complicated spectrum features and development of new applications based on this composite grating, such as MWFLs, high power fiber lasers and multi-parameter fiber sensors in harsh environment.

Acknowledgments

This work was supported by the National Natural Science Foundation of China (61505206, 61234004, 61376070, 61405190), the National Science and Technology Major Project of China (2016YFE0126800), and the Jilin Province Science and Technology Development Program (20150520089JH).

References

[1] K.O. Hill, G. Meltz, Fiber Bragg grating technology fundamentals and overview, J. Lightwave Technol. 15 (8) (1997) 1263–1276.
[2] J.L. Archambault, S.G. Grubb, Fiber gratings in lasers and amplifiers, J. Lightwave Technol. 15 (8) (1997) 1378–1390.
[3] Z. Zang, All-optical switching in Sagnac loop mirror containing an ytterbium-doped fiber and fiber Bragg grating, Appl. Opt. 52 (23) (2013) 5701–5706.
[4] Z. Zang, Y. Zhang, Analysis of optical switching in a Yb^{3+}-doped fiber Bragg grating by using self-phase modulation and cross-phase modulation, Appl. Opt. 51 (16) (2012) 3424–3430.

[5] C.R. Giles, Lightwave applications of fiber Bragg gratings, J. Lightwave Technol. 15 (8) (1997) 1391–1404.
[6] A. Othonos, X. Lee, R.M. Measures, Superimposed multiple Bragg gratings, Electron. Lett. 30 (23) (1994) 1972–1974.
[7] B.J. Eggleton, P.A. Krug, L. Poladian, F. Ouellette, Long periodic superstructure Bragg gratings in optical fibres, Electron. Lett. 30 (19) (1994) 1620–1622.
[8] C. Waltermann, A. Doering, M. Köhring, M. Angelmahr, W. Schade, Cladding waveguide gratings in standard single-mode fiber for 3D shape sensing, Opt. Lett. 40 (13) (2015) 3109–3112.
[9] R. Suo, J. Lousteau, H. Li, X. Jiang, K. Zhou, L. Zhang, W.N. MacPherson, H.T. Bookey, J.S. Barton, A.K. Kar, A. Jha, I. Bennion, Fiber Bragg gratings inscribed using 800 nm femtosecond laser and a phase mask in single-and multi-core mid-IR glass fibers, Opt. Express 17 (9) (2009) 7540–7548.
[10] R.R. Gattass, E. Mazur, Femtosecond laser micromachining in transparent materials, Nat. Photonics 2 (2008) 219–225.
[11] M. Malinauskas, A. Žukauskas1, S. Hasegawa, Y. Hayasaki, V. Mizeikis, R. Buividas, S. Juodkazis, Ultrafast laser processing of materials: from science to industry, Light: Sci. Appl. 5 (2016) e16133.
[12] C. Voigtländer, R.G. Becker, J. Thomas, D. Richter, A. Singh, A. Tünnermann, S. Nolte, Ultrashort pulse inscription of tailored fiber Bragg gratings with a phase mask and a deformed wavefront, Opt. Mater. Express 1 (4) (2011) 633–642.
[13] S.J. Mihailov, D. Grobnic, C.W. Smelser, P. Lu, R.B. Walker, H. Ding, Bragg grating inscription in various optical fibers with femtosecond infrared lasers and a phase mask, Opt. Mater. Express 1 (4) (2011) 754–765.
[14] J. Thomas, C. Voigtländer, R. Becker, D. Richter, A. Tünnermann, S. Nolte, Femtosecond pulse written fiber gratings: a new avenue to integrated fiber technology, Laser Photonics Rev. 6 (6) (2012) 709–723.
[15] M. Wang, J.T. Lin, Y.X. Xu, Z.W. Fang, L.L. Qiao, Z.M. Liu, W. Fang, Y. Cheng, Fabrication of high-Q microresonators in dielectric materials using a femtosecond laser: Principle and applications, Opt. Commun. 395 (2017) 249–260.
[16] K.K.C. Lee, A. Mariampillai, M. Haque, B.A. Standish, V.X.D. Yang, P.R. Herman, Temperature-compensated fiber-optic 3D shape sensor based on femtosecond laser direct-written Bragg grating waveguides, Opt. Express 21 (20) (2013) 24076–24086.
[17] B. Malo, K.O. Hill, F. Bilodeau, D.C. Johnson, J. Albert, Point-by-point fabrication of micro-Bragg gratings in photosensitive fibre using single excimer pulse refractive index modification techniques, Electron. Lett. 29 (18) (1993) 1668–1669.
[18] A. Martinez, M. Dubov, I. Khrushchev, I. Bennion, Direct writing of fibre Bragg gratings by femtosecond laser, Electron. Lett. 40 (19) (2004) 1170–1172.
[19] Y. Lai, K. Zhou, K. Sugden, I. Bennion, Point-by-point inscription of first-order fiber Bragg grating for C-band applications, Opt. Express 15 (26) (2007) 18318–18325.
[20] G.D. Marshall, R.J. Williams, N. Jovanovic, M.J. Steel, M.J. Withford, Point-by-point written fiber-Bragg gratings and their application in complex grating designs, Opt. Express 18 (19) (2010) 19844–19859.
[21] R.J. Williams, C. Voigtländer, G.D. Marshall, A. Tünnermann, S. Nolte, M.J. Steel, M.J. Withford, Point-by-point inscription of apodized fiber Bragg gratings, Opt. Lett. 36 (15) (2011) 2988–2990.
[22] C. Zhang, Y. Yang, C. Wang, C. Liao, Y.P. Wang, Femtosecond-laser-inscribed sampled fiber Bragg grating with ultrahigh thermal stability, Opt. Express 24 (4) (2010) 3981–3988.
[23] C. Hnatovsky, D. Grobnic, S.J. Mihailov, Through-the-coating femtosecond laser inscription of very short fiber Bragg gratings for acoustic and high temperature sensing applications, Opt. Express 25 (21) (2017) 25435–25446.
[24] J. Thomas, N. Jovanovic, R.G. Becker, G.D. Marshall, M.J. Withford, A. Tunnermann, S. Nolte, M.J. Steel, Cladding mode coupling in highly localized fiber Bragg gratings: modal properties and transmission spectra, Opt. Express 19 (1) (2010) 325–341.
[25] C. Koutsides, K. Kalli, D.J. Webb, L. Zhang, Characterizing femtosecond laser inscribed Bragg grating spectra, Opt. Express 19 (1) (2010) 342–352.
[26] H. Chikh-Bled, K. Chah, Á. González-Vila, B. Lasri, C. Caucheteur, Behavior of femtosecond laser-induced eccentric fiber Bragg gratings at very high temperatures, Opt. Lett. 41 (17) (2016) 4048–4051.
[27] M.L. Aslund, N. Jovanovic, N. Groothoff, J. Canning, G.D. Marshall, S.D. Jackson, A. Fuerbach, M.J. Withford, Optical loss mechanisms in femtosecond laser-written point-by-point fibre Bragg gratings, Opt. Express 16 (18) (2008) 14248–14254.
[28] N. Jovanovic, J. Thomas, R.J. Williams, M.J. Steel, G.D. Marshall, A. Fuerbach, S. Nolte, A. Tunnermann, M.J. Withford, Polarization-dependent effects in point-by-point fiber Bragg gratings enable simple, linearly polarized fiber lasers, Opt. Express 17 (8) (2009) 6082–6095.
[29] N. Jovanovic, A. Fuerbach, G.D. Marshall, M.J. Withford, S.D. Jackson, Stable high-power continuous-wave Yb^{3+}-doped silica fiber laser utilizing a point-by-point inscribed fiber Bragg grating, Opt. Lett. 32 (11) (2007) 1486–1488.
[30] R.J. Williams, N. Jovanovic, G.D. Marshall, G.N. Smith, M.J. Steel, M.J. Withford, Optimizing the net reflectivity of point-by-point fiber Bragg gratings: the role of scattering loss, Opt. Express 20 (12) (2012) 13451–13456.